Mathematical Biosciences and Engineering

MBE, 18(3): 2442–2454.
DOI: 10.3934/mbe.2021124
Received: 06 January 2021
Accepted: 08 March 2021
Published: 12 March 2021

http://www.aimspress.com/journal/MBE

Research article

Simulated biomechanical effect of aspheric transition zone ablation profiles after conventional hyperopia refractive surgery

Ruirui Du, Lihua Fang*, Binhui Guo, Yinyu Song, Huirong Xiao, Xinliang Xu and Xingdao He

Key Laboratory of Nondestructive Test (Ministry of Education), Nanchang Hangkong University, Nanchang 330063, China

*** Correspondence:** Email: fanglh71@126.com; Tel: +8618170938193.

Abstract: We studied the effects of the aspheric transition zone on the optical wavefront aberrations, corneal surface displacement, and stress induced by the biomechanical properties of the cornea after conventional laser in situ keratomileusis (LASIK) refractive surgery. The findings in this study can help improve visual quality after refractive surgery. Hyperopia correction in 1–5D was simulated using five types of aspheric transition zones with finite element modeling. The algorithm for the simulations was designed according to the optical path difference. Wavefront aberrations were calculated from the displacements on the anterior and posterior corneal surfaces. The vertex displacements and stress on the corneal surface were also evaluated. The results showed that the aspheric transition zone has an effect on the postoperative visual quality. The main wavefront aberrations on the anterior corneal surface are defocus, y-primary astigmatism, x-coma, and spherical aberrations. The wavefront aberrations on the corneal posterior surface were relatively small and vertex displacements on the posterior corneal surface were not significantly affected by the aspheric transition zone. Stress analysis revealed that the stress on the cutting edge of the anterior corneal surface decreased with the number of aspheric transition zone increased, and profile #1 resulted in the maximum stress. The stress on the posterior surface of the cornea was more concentrated in the central region and was less than that on the anterior corneal surface overall. The results showed that the aspheric transition zone has an effect on postoperative aberrations, but wavefront aberrations cannot be eliminated. In addition, the aspheric transition zone influences the postoperative biomechanical properties of the cornea, which significantly affect the postoperative visual quality.

Keywords: aspheric; transition zone; biomechanics; refractive surgery; cornea

1. Introduction

With the wide application of laser refractive surgery technology, a growing number of scholars have begun to pay attention to the postoperative visual quality. Some scholars have shown that the sphericity of the cornea is the main factor in the visual quality after conventional surgery [1,2]. During laser in situ keratomileusis (LASIK) refractive surgery, the design of the transition zone can reduce the spherical tendency of the cornea, facilitating better visual quality [3]. In order to better understand the effects of the transition zone on visual quality after refractive surgery, we studied the effects of different aspheric transition zones on the optical wavefront aberrations, vertex displacements, and stress distribution induced by the biomechanical properties of the cornea after LASIK refractive surgery.

The transition zone was designed to smooth the transition from the optical zone to the untreated cornea [4,5]. The aspheric transition zone used for refractive surgery requires serious consideration to avoid vision problems [6]. Fang et al. [5] indicated that the effect of the transition zone in refractive surgery should be taken into account while planning the surgery. If there is no smooth transition to the ablation edge in the ablation profile, mutations can occur between the ablation and untreated zones in the cornea [7,8]. Michael J. Endl et al. [9] reported that the results after photorefractive keratectomy with a transition zone were more physiological than those with no transition zone. Iben B. Damgaard et al. [10] compared the centration and functional optical zones after small incision lenticule extraction (SMILE) and LASIK. The treatment area during the study also included the transition zone.

There are many ways to design the ablation profile for the transition zone and the shape, size, and profile of the zone affect the postoperative visual quality. Some scholars indicated that a well-designed ablation profile for the aspheric transition zone can produce better safety and visual quality after refractive surgery [11,12]. Yoshiko Hori-komai et al. [13] compared a new ablation algorithm, termed the optimized aspheric transition zone, with refractive surgery for the correction of myopic astigmatism and found that patients treated with the former approach had better visual quality. Mohamed Hantera [14] investigated the effects of the transition zone on higher-order wavefront aberrations after LASIK using two kinds of aspheric transition zones algorithms.

Laser refractive surgery for that involves cutting the stromal layer will affects the integrity of the cornea and the biomechanical effects can subsequently damage the eye tissue. According to Miltos Balidis [15], the impact of corneal biomechanics are increasingly recognized as an influential factor on refractive surgery outcomes. Corneal biomechanical properties are of major importance in laser refractive surgery and must be taken into consideration to reduce the risk of iatrogenic ectasia. G. V. Vornin et al. [16] indicated that keratorefractive surgery affects corneal biomechanics. Dmitry Franus investigated the stress-strain changes in the cornea by modeling the cornea as a four-layer transversely isotropic shell with variable thickness and different biomechanical properties [17]. Magadalena Asejczyk-Widicka et al. [18] used the finite element method to simulate the process of refractive surgery in order to study the biomechanical and geometric parameters of the eyes. Irene Simonini et al. [19] estimated the corneal strain and stress in preoperative and postoperative configurations by creating a patient-specific solid model. Kalle Salmenhaara showed that when a part of the cornea is removed, the optical and biomechanical properties change accordingly [20].

This study aimed to evaluate the effects of five types of aspheric transition zones on visual quality after 1–5D hyperopia correction. The cutting depth for the aspheric transition zones (#1–5)

decreased gradually and the observed effects on the corneal biomechanics differed. The five aspheric transition zones were designed based on the optical zone used for conventional LASIK refractive surgery and the human eye model was constructed with finite element modeling. Material fitting, meshing, intraocular pressure (IOP) of 15 mmHg, and boundary conditions were performed in the finite element analysis software ANSYS. The optical wavefront aberrations, vertex displacements, and stress were also calculated. The effects of the five aspheric transition zones on the biomechanical properties of the cornea were analyzed. The results have significance for clinical refractive surgery and the improvement of postoperative visual quality.

2. Methods

2.1. Simulation of conventional LASIK refractive surgery

In order to simulate the conventional refractive surgery, a 3D solid model was first constructed using the 3D modeling software NX based on the average geometry of human eye. The central corneal thickness is 0.5 mm, the curvature radius of anterior corneal surface is 7.7 mm, and the curvature radius of posterior corneal surface is 6.8 mm. According to the normal values of anatomy and physiology, the horizontal diameter of sclera is 23.5 mm, the vertical diameter is 23 mm. Then, a finite element model of the human eye was created in the finite element analysis software ANSYS. First, the corneal flap was created in the finite element model, and its thickness was uniform. Then the stroma layer under the flap was cut. Different hyperopia correction has different cutting depth. This is the process of refractive surgery simulation.

After the finite element model was created, it is necessary to add materials to the tissue in ANSYS. The cornea and sclera were considered to be directly connected. According to the nonlinear material properties of cornea and sclera, we use the hyperelastic material model based on Ogden function. The strain energy function can be expressed as:

$$W = \sum_{k=1}^{N} \frac{1}{d_k} (J-1)^{2k} + \sum_{i=1}^{N} \frac{\mu_i}{\alpha_i} (\bar{\lambda}_1^{\alpha_i} + \bar{\lambda}_2^{\alpha_i} + \bar{\lambda}_3^{\alpha_i} - 3) \tag{1}$$

where W represents the strain energy function. N, μ_i, α_i, and d_k are the material constants. $\overline{\lambda_p} = J^{-\frac{1}{3}}\lambda_p$ is the elongation corresponding to the principal direction. λ_p indicates the left Cauchy-Green tensor of principal elongation. λ shows the determinant of the elastic deformation gradient.

In the process of material fitting, we choose $N = 2$ and $N = 1$ as the fitting order of cornea and sclera. The corneal fitting parameters were: α_1= 103.51, μ_1= 0.003535 MPa, α_2= 103.61. μ_2= 0.003535 MPa. The fitting parameters of sclera were: α_1= 182.73, μ_1= 0.030224 MPa.

The initial bulk modulus k can defined as:

$$k = \frac{2}{d_1} \tag{2}$$

The initial shear modulus μ is defined as follows:

$$\mu = \frac{1}{2} \sum_{i=1}^{N} \alpha_i \mu_i \tag{3}$$

After adding materials, meshes for each component of the model were divided in ANSYS. Since our research was focused on the cornea, the mesh for the cornea was thinner than that for the sclera. The cornea and sclera were divided into different-sized hexahedral meshes based on their shape and characteristics. Figure 1 shows the local schematic diagram of the human eye model after meshing; in the figure, the mesh for the cornea is clearly thinner than that for the sclera.

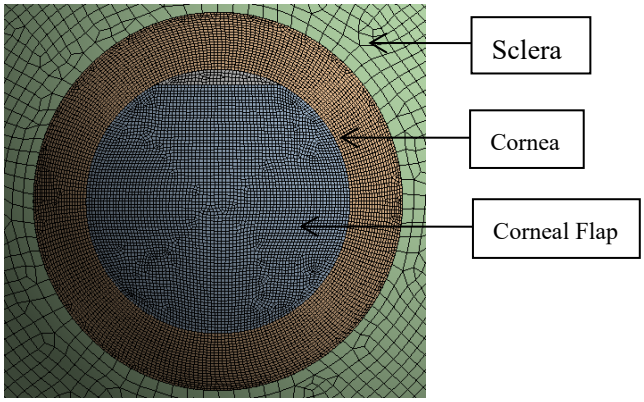

Figure 1. Local schematic diagram of finite element model of human eye after meshing.

We simulated the correction of 1–5D pure hyperopia. Each of the 1–5D models was designed with a different profile for the aspheric transition zone. The thickness of the corneal flap was 100 um and the diameter was 8 mm, the diameter of the optical zone was 6 mm, and the width of the transition zone was 1.05 mm.

2.2. Aspheric transition zone in conventional refractive surgery

In this study, five types of ablation profiles were designed, with a smooth transition from the optical zone edge to the unaltered cornea. The aspheric transition zone has been widely demonstrated proved to be safe and predictable. The aspheric ablation profile can be defined as:

$$d(x,y) = f_b(x,y).d_e(x,y) \tag{4}$$

here

$$d_e(x,y) = f\left(\frac{O_z x}{2\sqrt{x^2+y^2}}, \frac{O_z y}{2\sqrt{x^2+y^2}}\right) \tag{5}$$

This formula defines the extended ablation depth of the transition region, which extends from the boundary value of the optical zone. O_z represents the diameter of the optical zone.

In addition, $f_b(x,y)$ is the blend function for the aspheric ablation algorithm and provides the normalized ablation depth for the transition zone. The value of this function is 1 between the optical zone and the transition zone, but changes to 0 at the boundary between the transition zone and the untreated periphery. Before the blend function is achieved, an aspheric ablation function must be created as follows:

$$f_b^{'}(x,y) = h - \frac{(x^2+y^2)}{R+[R^2-(x^2+y^2)(Q+1)]^{1/2}} \tag{6}$$

or

$$f_b^{'}(x,y) = \frac{[x_0-(x^2+y^2)^{1/2}]^2}{R+\{R^2-[x_0-(x^2+y^2)^{1/2}]^2(Q+1)\}^{1/2}} \tag{7}$$

here, h is the non-zero value of the ablation depth at the edge of the optical zone and x_0 represents the width of the transition zone. Q represents the asphericity and R represents the curvature radius of the ablation profile. The value of R can be calculated as follows:

$$R = \frac{(x_0)^2+h^2(1+Q)}{2h} \tag{8}$$

Then, the aspheric blend function can be obtained by normalization method:

$$f_b(x,y) = f_b^{'}(x,y)/h \tag{9}$$

In this study, five types of ablation profiles for the aspheric transition zone (from #1 to #5) were designed by changing the Q value. The relationship of the normalized aspheric blend function to the transition zone width is shown in Figure 2. The vertical axis represents the depth of normalized ablation and the horizontal axis represents the normalized vertical distance from the ablation point in the transition zone to the edge of the optical zone.

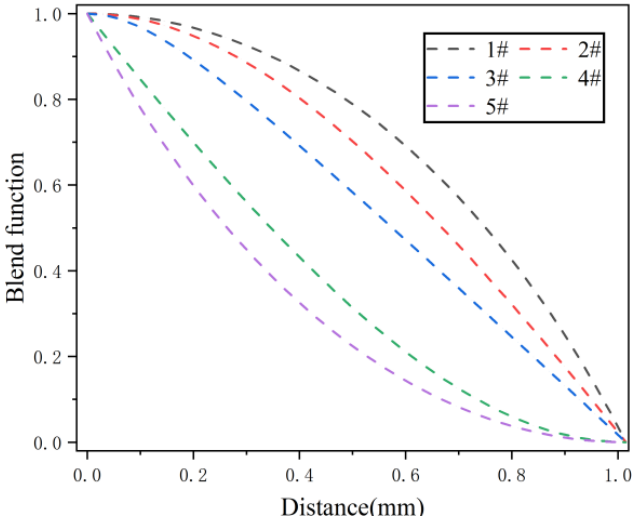

Figure 2. Five types of aspheric ablation profiles for transition zone are described. The corresponding Q values for the profiles from profile #1 to profile #3 are 20, -30 and -80, the corresponding Q values for the profiles from profile #4 to profile #5 are -30 and 20. Here, h = 0.1 mm, the width of transition zone was 1.05 mm.

2.3. The influences of biomechanical properties on refractive surgery

During the LASIK refractive surgery, destruction of the integrity of the cornea is inevitable. By calculating the depth of corneal ablation in the optical zone and the transition zone, corneal stromal ablation during refractive surgery was simulated. The corneal flap and stroma surfaces were created and a finite element model of the human eye was constructed using NX software. The creation of the corneal flap and the cutting of the stromal layer all affect the integrity of the cornea and can induce a change in corneal morphology, resulting in the displacement of the corneal surface. The refractive state of the cornea eventually changes, mainly due to the aberrations and displacements caused by the biomechanical properities after LASIK. We evaluated the effects of the aspheric transition zone on the residual optical wave-front aberrations, the increase in vertex displacements, and the stress on the corneal surface after conventional LASIK hyperopia refractive surgery.

3. Results

3.1. The effects of the aspheric profile for the transition zone on optical wavefront aberrations after conventional LASIK refractive surgery

We assumed that there was no decentration during refractive surgery can also did not take astigmatism into account. Wave-front aberrations were calculated from corneal surface displacements according to the algorithm designed with an optical path difference. The Zernike coefficient was obtained by mathematical fitting. The preoperative and postoperative aberrations were all expressed as six-order Zernike polynomials and the residual wave-front aberrations were calculated as the difference between the preoperative and postoperative aberrations. We investigated the relationship between the aberrations caused by the x, y, and z-axis displacements from the aspheric transition zone and the diopter.

3.1.1. Wave-front aberrations caused by displacement of anterior corneal surface

Ablation of part of the corneal stroma leads to a decrease in the corneal thickness during conventional LASIK refractive surgery. Under IOP, the anterior and posterior surfaces of the cornea are displaced, altering the refractive state of the cornea. By calculating the displacements in the corneal surface, the displacements were transformed into Zernike coefficients to obtain the wave-front aberrations. Firstly, the effects of different aspheric profiles for the transition zone on the aberrations induced by anterior corneal surface displacements were evaluated. Figure 3 depicts the defocus (C_2^0), y-primary astigmatism (C_2^2), x-coma (C_3^{-1}), and spherical aberration (C_4^0) values. The other aberrations were small and were therefore not calculated.

Figure 3(A) shows the defocus. It can be seen from the figure that the ablation profiles for the aspheric transition zone had an influence on the defocus. When the degree of hyperopia correction remained constant, the defocus value decreased as the number of aspheric transition zone increased. Profile #1 resulted in the maximum defocus value, and 5D hyperopia correction with profile #1 produced the maximum defocus value, which was 1.25 mm. Figure 3(B) shows the x-coma. It can be seen from the image that the transition zone had little effect on the x-coma value, which was small. In addition, the negative x-coma value increased as the hyperopia diopter increased. The y-coma value was less than 0.01 and was therefore not reported. The y-coma was small due to the direction

of the corneal flap pedicle. Figure 3(C) shows y-primary astigmatism. The image shows that the different aspheric transition zones had no obvious influence on the y-primary astigmatism value, which was small. In addition, the y-primary astigmatism increased gradually as the diopter increased. The value of the x-primary astigmatism was less than 0.01; this was also due to the direction of the corneal flap pedicle. Figure 3(D) shows the spherical aberration, which increased in a negative direction as the number of aspheric transition zone and the diopter increased. The above results indicate that the aspheric transition zone has an effect on postoperative wave-front aberrations and the depth of cutting can affect the biomechanical properties of the cornea.

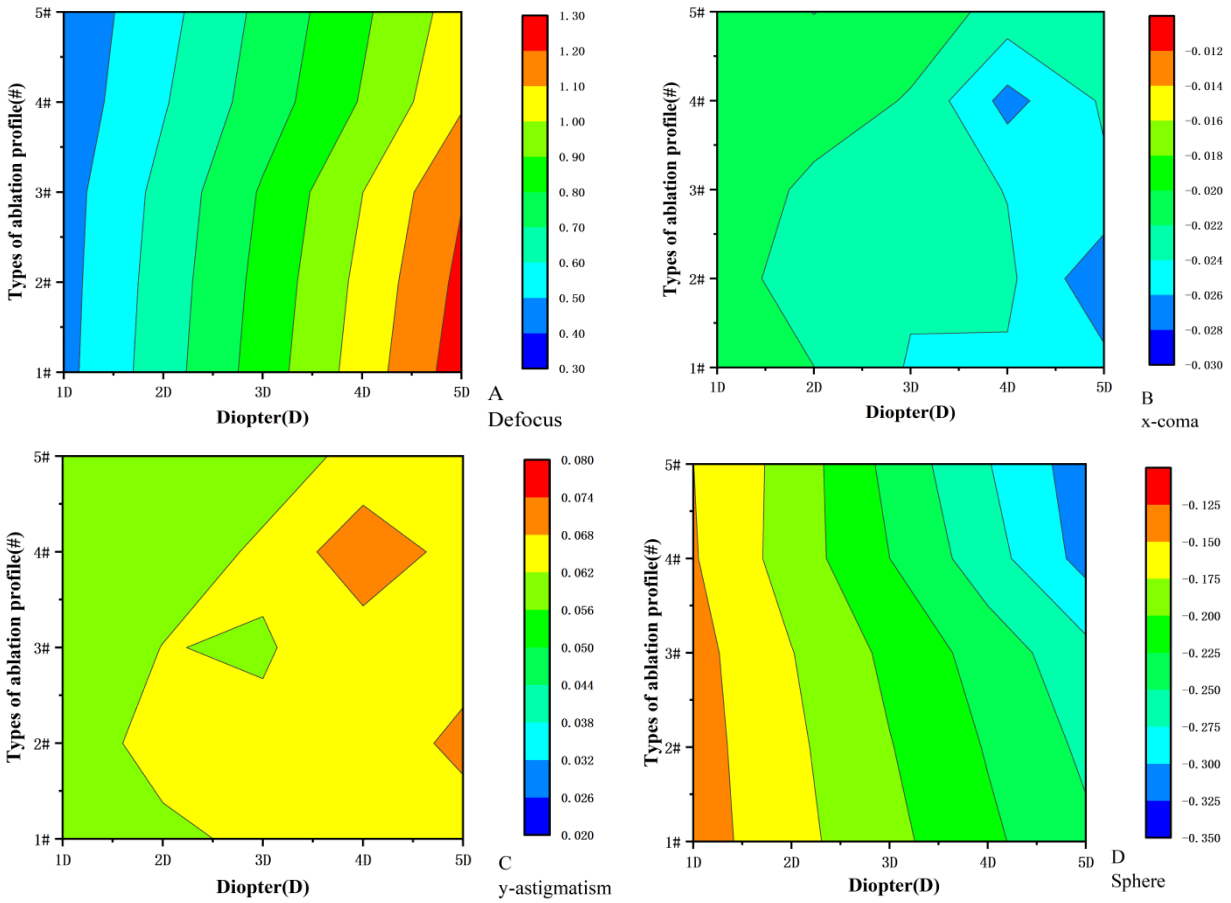

Figure 3. This figure shows some wavefront aberrations caused by displacement of anterior corneal surface, we can see that defocus and spherical aberrations have strong regularity. The optical zone is 6mm and the width of transition zone is 1.05 mm.

3.1.2. Wave-front aberrations induced by displacements of posterior corneal surface

Using the above method, the wavefront aberrations caused by the displacement of the posterior corneal surface were determined. The results showed that the wavefront aberrations caused by the displacement of the posterior corneal surface were small overall. We only assessed the changes in some wavefront aberrations as the other aberrations were too small to consider. Figure 4 depicts the partial aberrations on the posterior corneal surface, with the defocus presented in Figure 4(A) and spherical aberration in Figure 4(B).

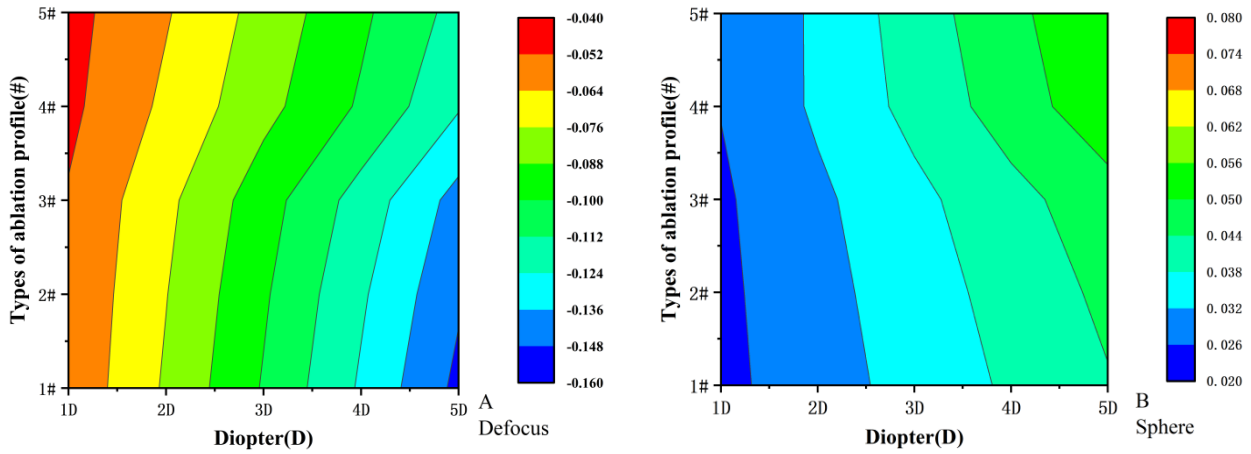

Figure 4. The wavefront aberrations induced by the displacements of the posterior corneal surface were described, the other aberrations were small. We can know from Figure 3 that the defocus and spherical aberrations of the posterior are about 1 / 8-1 / 7 of the anterior corneal surface.

Figure 4(A) shows that the defocus value decreased in the negative direction if the number of aspheric transition zone increased while the diopter remained constant. The diopter was inversely proportional to the defocus. 5D hyperopia correction with profile #1 produced the maximum negative defocus value of -0.15 mm (Figure 4(B)). Spherical aberrations increased with the number of aspheric transition zone increased. Spherical aberrations were directly proportional to the diopter and the 5D hyperopia correction with profile #5 produced the maximum value for spherical aberrations, which was 0.056 mm.

3.2. The influence of the aspheric profile for the transition zone on posterior corneal surface vertex displacements

In the finite element analysis software, an IOP of 15 mmHg was applied to the finite element model of the human eye and the preoperative and postoperative deformations in the cornea were analyzed. Under IOP, the cornea was significantly deformed, whereas the scleral deformation was small. However, there was a significant deformation at the junction of the cornea and sclera. The deformation was largest on the incision side of the corneal flap due to the separation of the stromal layer from the flap. Because IOP affects the inner surface of the cornea directly, we speculated that the deformation on the posterior surface of the cornea is greater than that on the anterior corneal surface. Therefore, we focused on the effect of the aspheric transition zone on the displacement of the posterior corneal surface. The increase in the vertex displacement is the difference between the preoperative and postoperative maximum values of the posterior corneal surface and it represents the displacement of the center of the cornea relative to the edge; therefore it is also a relative value.

Figure 5 shows that the effect of the aspheric transition zone on the vertex displacement of the posterior surface was not obvious; however, the vertex displacement decreased slowly as the number of aspheric transition zone increased. In addition, the vertex displacement also increased with the increase of the diopter, and 5D hyperopia correction with profile #5 produced the maximum value, which was 23 um. Similarly, we calculated the increase in vertex displacement in the anterior corneal surface. The value was relatively small and will not be discussed.

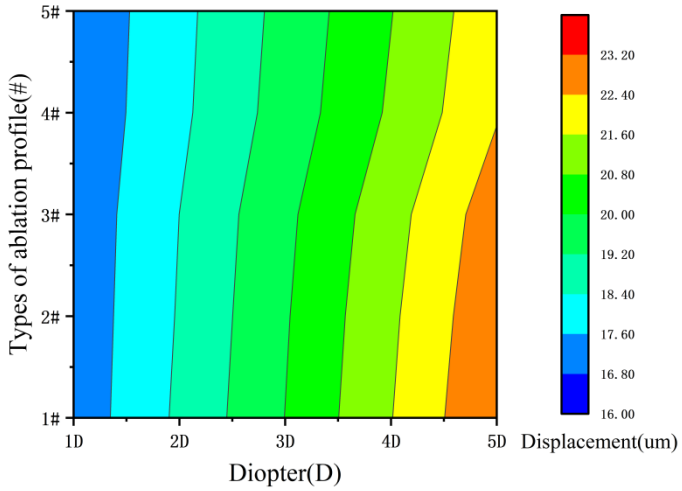

Figure 5. The vertex displacements of the posterior corneal surface was demonstrated. The x-axis represents the diopter correction degree of hyperopia, and the y-axis represents the ablation profile of aspheric transition zone.

3.3. Effect of aspheric transition zone on postoperative corneal surface stress

The biomechanical stress on the cornea decreases after LASIK refractive surgery. A thin corneal flap is helpful to maintain the original stress on the cornea and the cutting depth affects the stress and corneal deformation. Different ablation profiles for the aspheric transition zone may lead to different stress changes in the optical and untreated zones. Figure 6 shows the relationship between the aspheric transition zone and the corneal surface stress after 4D hyperopia refractive correction.

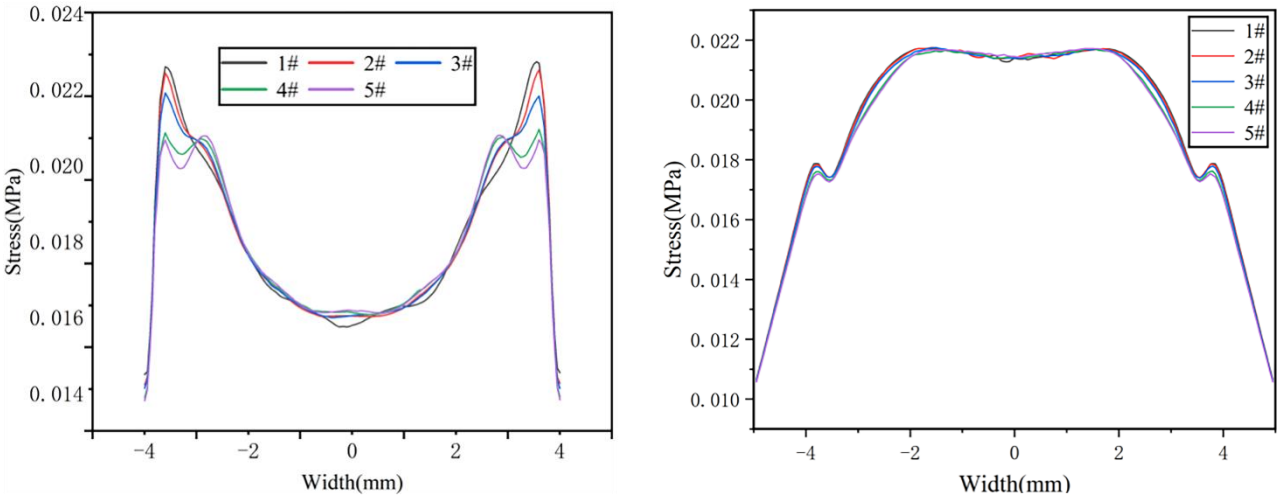

A B

Figure 6. The distribution of stress on the anterior and posterior surface of cornea was described. A shows the distribution of stress on the anterior corneal surface, B shows the distribution of stress on the posterior corneal surface.

Figure 6(A) shows that the different aspheric transition zones had very little influence on the stress in the central zone, but significantly affected the stress in the value edge area. Profile #1 resulted in maximum stress because this profile had the largest edge zone which had a substantial influence on the corneal biomechanics. The figure shows that the peak stress was located near abscissa -3 and was caused by the incision on the corneal flap. Peak stress also appeared near abscissa + 3, caused by the incision at edge of the corneal flap. The stress at these two locations increased as the number of aspheric transition zone increased. Figure 6(B) shows that the aspheric transition zone did not significantly affect the stress on the posterior corneal surface, which showed no significant changes as the number of aspheric transition zone increased. The stress in the central region was larger and a small peak appeared at the point with the peak stress on the anterior corneal surface. In addition, the stress on the corneal posterior surface was less than that on the anterior surface.

4. Discussion

Second to fourth-order Zernike coefficients were used in this study and smaller coefficients were not considered. Tian et al. [21] have indicated that high order aberration is an important factor affecting the retinal imaging, study on the relationship between higher order aberrations and contrast sensitivity can provide some theoretical guidance for clinical surgery refractive doctor. The use of an individualized elliptical transition maximizes the circular effective optical zone and can enhance the smoothness of the transition zone while minimizing excessive tissue removal [4]. Many studies have shown that the visual quality after refractive surgery can be improved by optimizing the design of the transition zone and that wavefront aberrations after refractive surgery with a transition zone are less than those without a transition zone. Hyperopic treatment normally increases corneal eccentricity, aspheric transition zones can reduce corneal eccentricity [22]. D. Epstein et al. [23] treated sixtyfive eyes of 46 patients with hyperopia ranging from +1.00 D to +9.00 D, they found that the aspheric algorithm appears to provide excellent predictability and refractive stability for hyperopia. The differences between the five types of aspheric transition zones designed in this study lay in the cutting depth of the cornea. Profile #1 had the largest cutting depth, which resulted in a thick corneal flap. Different degrees of refractive correction can be achieved with different thickness values for the stromal bed. In theory, a thinner corneal flap is more helpful to maintain the original biomechanical properties of the cornea. Dong et al. [24] indicated that thin flaps are helpful for maintaining the original stress. This may be because a thinner corneal flap cause less damage to the corneal integrity. In this study, we found that postoperative wave-front aberrations led to changes in the defocus, spherical aberrations, and coma. The transition zone was designed to smooth the transition from the optical surface to the untreated cornea and mainly dominated the induced coma and spherical wavefront aberrations [5]. According to our results for the stress, at the cutting edge, profile #1 resulted in the maximum stress and the stress induced by profiles #2–5 decreased in turn. Refractive surgery changes the shape of the cornea. The cornea moves forward to a certain extent after surgery, which affects its properties [25]. In this paper, IOP was a fixed value, which is 15 mmHg. IOP may affect the outcome of refractive surgery, in our paper, the effects of IOP on hyperopia correction was not considered. However, we have studied the effect of IOP on myopia correction. IOP has effects on corneal surface displacement, aberrations and stress after refractive surgery. Lanchares et al. [26] analyzed the effects of IOP on the refractive correction. Many other factors also affect the postoperative visual quality during refractive correction [25,27].

5. Conclusions

By simulating the conventional LASIK pure hyperopia correction, the effects of the aspheric transition zone on the biomechanics were evaluated. The results showed that the aspheric transition zone affects the postoperative visual quality. The main wavefront aberrations on the anterior corneal surface were defocus, y-primary astigmatism, x-coma, and spherical aberrations. The aberrations on the corneal posterior surface were relatively small. The vertex displacements on the posterior corneal surface were not significantly affected by the aspheric transition zone, but the values increased as hyperopia correction diopter increased. Stress analysis revealed that the stress on the cutting edge of the anterior corneal surface decreased as the the number of aspheric transition zone increased and profile #1 resulted in the maximum stress. The stress on the posterior surface of the cornea was more concentrated in the central region and was lower than that on the anterior corneal surface overall. The aspheric transition zone influenced the postoperative optical wave-front aberrations and biomechanical effect of cornea after refractive surgery. The aspheric transition zone had a positive effect on postoperative aberrations, but wave-front aberrations could not be eliminated. In addition, the biomechanical effect of the cornea tissue had an important effect on the postoperative visual quality.

Acknowledgments

Supported by the Natural National Science Foundation of China (NSFC) (61465010 & 81873684), the National Key Research and Development Program of China (2018YFE0115700) and Jiangxi Nature Science Foundation (20192BAB207035). The authors alone are responsible for the content and writing of the article.

Conflicts of interest

All authors declare no conflicts of interest in this paper.

References

1. Z. W. Shen, H. Z. Zhou, H. Yin, J. T. Wu, L. Li, Fine adjusted-customized ablation LASIK treatment for myopia, *Int. J. Ophthalmol.*, **5** (2005), 1194–1197.
2. Z. J. Fan, S. J. Xu, Z. H. Jia, B. C. Liu, Clinical significance of corneal Q value in myopic patients, *Int. J. Ophthalmol.*, **6** (2006), 642–643.
3. X. U. Li, Q. Tao, L. Y. Zhuang, Visual outcome after optimized aspheric transitionzone laser keratomileusis compared toconventional LASIK, *Int. Eye Sci.*, **7** (2007), 623–625.
4. S. MacRae, Excimer ablation design and elliptical transition zones, *J. Cataract Refractive Surg.*, **25** (1999), 1191–1197.
5. L. Fang, Y. Wang, X. He, Theoretical analysis of wavefront aberration caused by treatment decentration and transition zone after custom myopic laser refractive surgery, *J. Cataract Refractive Surg.*, **39** (2013), 1336–1347.
6. G. M. Dai, Application of complementary error function to the transition zone of myopic ablation shapes in refractive surgery, *J. Appl. Math. Phys.*, **5** (2017), 1521–1528.
7. E. Gross, R. Hofer, J. Wong, Application of blend zones, depth reduction, and transition zones to ablation shapes, Patent No. 8216213, 2012.

8. J. Shen, Y. Zhang, W. Liao, Mathematical model based corneal toric surface for excimer laser refractive surgery, *J. Southeast Univ.*, **36** (2006), 531–536.
9. M. J. Endl, C. E. Martinez, S. D. Klyce, M. B. McDonald, S. J. Coorpender, R. A. Applegate, et al., Effect of larger ablation zone and transition zone on corneal optical aberrations after photorefractive keratectomy, *Arch. Ophthalmol.*, **119** (2001), 1159–1164.
10. I. B. Damgaard, M. Ang, A. M. Mahmoud, M. Farook, C. J. Roberts, J. S. Mehta, Functional optical zone and centration following SMILE and LASIK: a prospective, randomized, contralateral eye study, *J. Refractive Surg.*, **35** (2019), 230–237.
11. A. P. Nisarta, D. Desai, K. Solanki, Corneal higher order aberrations after aspheric LASIK treatment, *Int. J. Health Sci. Res.*, **6** (2016), 107–113.
12. T. Gamaly, LASIK with the optimized aspheric transition zone and cross-cylinder technique for the treatment of astigmatism from 1.00 to 4.25 diopters, *J. Refractive Surg.*, **25** (2009), S927–930.
13. Y. H. Komai, I. Toda, N. A. Kato, M. Ito, T. Yamaoto, K. Tsubota, Comparison of LASIK using the NIDEK EC-5000 optimized aspheric transition zone (OATz) and conventional ablation profile, *J. Refractive Surg.*, **22** (2006), 546–555.
14. M. Hantera, Comparison of postoperative wavefront aberrations after NIDEK CXIII optimized aspheric transition zone treatment and OPD-guided custom aspheric treatment, *J. Refractive Surg.*, **25** (2009), S922–926.
15. M. Balidis, Biomechanical profile of refractive surgery procedures, *Acta Ophthalmol.*, **97** (2019).
16. G. V. Voronin, I. A. Bubnova, Changes in biomechanical properties of the cornea after keratorefractive surgery, *Vestn. Oftalmologii*, **135** (2019), 108–112.
17. D. V. Franus, Change in the stress-strain state of the cornea after refractive surgery, in *International Conference on Mechanics-seventh Polyakhovs Reading*, *IEEE*, (2015), 1–4.
18. M. A. Widlicka, W. Srodka, P. K. Berkowska, The biomechanical modelling of the refractive surgery, *Optik*, **120** (2009), 923–933.
19. I. Simonini, A. Pandolfi, Customized finite element modelling of the human cornea, *PloS one*, **10** (2015), e0130426.
20. K. Salmenhaara, *Impact of Refractive Surgery to the Biomechanical Properties of the Cornea-a Finite Element Analysis*, Master thesis, Aalto University, 2015.
21. H. Y. Tian, B. Wang, J. X. Huo, Research progress of the effects of high order aberrations on visual quality after the LASIK, *Prog. Mod. Biomed.*, **14** (2014), 3393–3395.
22. P. Vinciguerra, F. I. Camesasca, Treatment of hyperopia: a new ablation profile to reduce corneal eccentricity, *J. Refractive Surg.*, **18** (2002), 315–317.
23. D. Epstein, P. Vinciguerra, M. Azzolini, P. Radiee, Long-term follow-up of hyperopic photorefractive keratectomy (prk) performed with a new algorithm, *Invest. Ophthalmol. Visual Sci.*, **38** (1997).
24. Z. X. Dong, X. T. Zhou, Advences in biomechanical effects of laser corneal refractive surgery, *Chin. J. Opthalmol.*, **48** (2012), 1053–1056.
25. J. Kim, Analysis of corneal higher-order aberrations after myopic refractive surgery, *Curr. Opt. Photonics*, **3** (2019), 72–77.
26. E. Lanchares, B. Calvo, M. A. D. Buey, J. A. Cristóbal, M. doblaré, The effect of intraocular pressure on the outcome of myopic photorefractive keratectomy: a numerical approach, *J. Healthcare Eng.*, **1** (2010), 461–476.

27. L. Fang, W. Ma, Y. Wang, Y. Dai, Z. Fang, Theoretical analysis of wave-front aberrations induced from conventional laser refractive surgery in a biomechanical finite element model, *Invest. Ophthalmol. Visual Sci.*, **61** (2020), 33–34.

AIMS Press